Published in final edited form as:
Mol Cell Neurosci. 2010 October ; 45(2): 92–100. doi:10.1016/j.mcn.2010.06.002.

The ARMS/Kidins220 scaffold protein modulates synaptic transmission

Juan Carlos Arévalo[1,2,*], **Synphen H. Wu**[1], **Takuya Takahashi**[3], **Hong Zhang**[4], **Tao Yu**[2], **Hiroko Yano**[1,7], **Teresa A. Milner**[5], **Lino Tessarollo**[6], **Ipe Ninan**[1], **Ottavio Arancio**[4], and **Moses V. Chao**[1,*]

[1]Molecular Neurobiology Program, Skirball Institute of Biomolecular Medicine, Departments of Cell Biology, Physiology and Neuroscience, and Psychiatry, New York University School of Medicine, New York, NY 10016, USA.

[2]Instituto de Neurociencias de Castilla y León (INCyL), Universidad de Salamanca, Salamanca 37007, Spain.

[3]Department of Physiology, Yokohama City University, Graduate School of Medicine 3-9 Fukuura Kanazawa-ku, Yokohama, Japan 236-0004.

[4]Department of Pathology, Taub Institute, Columbia University, New York, NY 10032, USA.

[5]Department of Neurology and Neuroscience, Weill Cornell Medical College, 407 East, 61st Street, New York, NY 10065, USA, and Laboratory of Neuroendocrinology, The Rockefeller University 12330 York Ave, New York, NY 10065, USA.

[6]Neural Development Group, Mouse Cancer Genetics Program, Center for Cancer Research, National Cancer Institute, Frederick, Maryland 21702, USA.

Abstract

Activity-dependent changes of synaptic connections are facilitated by a variety of scaffold proteins, including PSD-95, Shank, SAP97 and GRIP, which serve to organize ion channels, receptors and enzymatic activities and to coordinate the actin cytoskeleton. The abundance of these scaffold proteins raises questions about the functional specificity of action of each protein. Here we report that basal synaptic transmission is regulated in an unexpected manner by the ankyrin repeat-rich membrane-spanning (ARMS/Kidins220) scaffold protein. In particular, decreases in the levels of ARMS/Kidins220 *in vivo* led to an increase in basal synaptic transmission in the hippocampus, without affecting paired pulse facilitation. One explanation to account for the effects of ARMS/Kidins220 is an interaction with the AMPA receptor subunit, GluA1, which could be observed after immunoprecipitation. Importantly, shRNA and cell surface biotinylation experiments indicate that ARMS/Kidins220 levels have an impact on GluA1 phosphorylation and localization. Moreover, ARMS/Kidins220 is a negative regulator of AMPAR function, which was confirmed by inward rectification assays. These results provide evidence that modulation of ARMS/Kidins220 levels can regulate basal synaptic strength in a specific manner in hippocampal neurons.

[*]To whom correspondence should be addressed: arevalojc@usal.es; Moses.Chao@med.nyu.edu. .
[7]Present address: Department of Neurosurgery, Brigham and Women's Hospital, Harvard Medical School, 221 Longwood Avenue, Boston, MA 02115, USA.

Keywords

ARMS-Kidins220; scaffold; synaptic transmission

Introduction

Synaptic proteins containing PDZ domains or PDZ-binding motifs carry out multifaceted functions in regulating cytoskeletal remodeling of dendritic spines and in the trafficking of glutamate receptors. Scaffold proteins, such as PSD-95, PICK and Shank are abundantly expressed at the postsynaptic density and possess many well defined protein motifs, such as multiple ankyrin repeats, PSD95-DLG1-ZO1 (PDZ) domains; phosphotyrosine binding domain (PTB), SH3 domains, and sterile-alpha motif (SAM) domains, capable of multiple protein interactions. The most prominent interactions are with glutamate receptor channels, AMPA and NMDA, and potassium channels (Shin et al., 2000) and the Rho family of GTPases and their many effectors, the Rho-GEFs (Tada and Sheng, 2006). These interactions allow for scaffold proteins to simultaneously cluster signaling and receptor complexes and remodel dendritic spines in a dynamic manner.

One scaffold protein that is highly expressed in the hippocampus, the Ankyrin-rich membrane spanning (ARMS) or Kinase D-interacting substrate of 220kD (Kidins220) protein (referred to hereafter as ARMS), was originally identified as an interactor of p75 and Trk receptors (Kong et al., 2001) and is directly phosphorylated by protein kinase D (Iglesias et al., 2000) and Trk receptors (Arevalo et al., 2006; Arevalo et al., 2004; Kong et al., 2001). The ARMS protein has many of the characteristics of a scaffold protein in possessing 11 ankyrin repeats, a polyproline region, a SAM domain and a C-terminal PDZ-binding motif. As a transmembrane protein, ARMS is distinguished by four membrane spanning domains.

Previous work indicated that the levels of ARMS protein are regulated by neuronal activity. Chronic treatment with TTX, which prevents action potential firing, increased the levels of ARMS in mature rat hippocampal cultures, whereas chronic treatment with bicuculline, which blocks inhibitory GABAergic transmission, decreased ARMS levels (Cortes et al., 2007). Moreover, whole-cell voltage clamp recordings of rat hippocampal neurons indicated that these treatments produced changes in mEPSC amplitude and frequency (Cortes et al., 2007), suggesting that alterations in ARMS levels may modify glutamatergic neurotransmission. Analysis of mice deficient in the ARMS protein in the dentate gyrus and the barrel somatosensory cortex also indicated that ARMS can play a role in the refinement and stabilization of dendritic spines during postnatal development (Wu et al., 2009).

Although it has been proposed that ARMS may play a role as a homeostatic regulator of synaptic strength, the impact and mechanism of ARMS as a scaffold in synaptic physiology have not been studied. Here we show the levels of ARMS are critical to basal synaptic transmission in hippocampal neurons. Because alterations in activity influence AMPA receptor currents (Thiagarajan et al., 2005), we followed the distribution and phosphorylation of GluA1 as a function of ARMS levels. We find that changes in ARMS levels results in increases in GluA1 phosphorylation and cell surface insertion. Interestingly, an interaction exists between ARMS and GluA1 though their transmembrane domains. Our results demonstrate that ARMS/Kidins220 protein can modify basal synaptic transmission through mechanisms that involve the GluA1 subunit.

Results

Synaptic localization of ARMS

To address ARMS localization in primary neurons, we performed fractionation experiments using cultured hippocampal neurons to generate biochemical fractions enriched in intracellular membranes (Fig. 1A). In this experiment, ARMS co-migrated with Trk receptors in the same fractions (Fig. 1B), consistent with the previous reported data indicating an interaction between both proteins (Arevalo et al., 2006;Arevalo et al., 2004). These fractions were positive for EEA1, an established marker of early endosomes, and for GluA1 subunit, but not for ribophorin, an endoplasmic reticulum marker. The intracellular distribution of ARMS was confirmed by co-staining with EEA1 in hippocampal neurons with ARMS being present in 30 +/− 4.74% of EEA1-positive endomembranes (data not shown). Electron microscopy studies indicated that ARMS was localized to endomembranes near contacts or synapses from terminals in the CA1 region of the hippocampus (Fig. 1C, panels a and b). All together these data indicate that ARMS is in endomembranes close to synaptic areas.

ARMS protein levels modulate basal synaptic transmission

The ARMS protein has been found to be regulated during development by activity (Cortes et al., 2007). To test whether modulating ARMS has any effect upon hippocampal synaptic transmission, we generated an ARMS-deficient mouse strain (Wu et al., 2009). Although $ARMS^{-/-}$ mice die early *in utero*, $ARMS^{+/-}$ mice are viable and fertile. They exhibit normal brain morphology despite a 30–40% decrease of ARMS protein compared to wild-type mice (Wu et al., 2009). Using hippocampal slices, we tested if basal synaptic transmission in $ARMS^{+/-}$ mice was altered. Basal synaptic neurotransmission at Shaffer collateral-CA1 synapses in $ARMS^{+/-}$ mice at 1 month of age was significantly higher than wild-type animals (Fig. 2A). However, no differences were found in paired pulse facilitation (Fig. 2B), suggesting that the probability of neurotransmitter release from the presynaptic terminal is not affected by lowering ARMS levels.

ARMS modulates surface expression of GluA1

Insertion and removal of AMPARs into the synapses have been proposed as a mechanism to account for the ability of neurons to modify basal synaptic transmission and plasticity (Malinow and Malenka, 2002). To test whether changes in ARMS levels might influence GluA1 membrane expression, we used a biotinylation assay to measure GluA1 surface expression in hippocampal neurons. We used a lentivirus that expressed GFP and ARMS shRNA to reduce the level of ARMS (Cortes et al., 2007). The expression of the ARMS shRNA, but not control shRNA, could downregulate ARMS effectively (at least 80%), as demonstrated in cultured hippocampal neurons by western blot (Fig. 3A) and immunofluorescence analysis (Fig. 3B).

We found decreasing ARMS levels led to a 2-fold increase in GluA1 receptor levels at the cell surface, without affecting the total amount of the receptor, as measured by surface biotinylation followed by streptavidin pull-down and western blotting (Fig. 3C). No differences were observed in the levels of surface GluA2 (Fig. 3C). The specificity of surface labeling was assessed by the absence of tubulin immunoreactivity after streptoavidin pull-down. These data were further confirmed using immunofluorescence to detect surface levels of GluA1. Neurons transfected with a plasmid expressing GFP and ARMS shRNA produced an increase in cell surface GluA1 as compared to neurons expressing GFP and control shRNA (Fig. 3D, compare left and right panels). Quantification of the data indicated a 2.37-fold increase of surface GluA1 when ARMS was depleted (Fig. 3D), an increase that was similar to the one obtained using the biotinylation assay (Fig. 3C).

Decreases in ARMS protein resulted in increased GluA1 surface expression. To determine the effects of increasing ARMS protein levels, we transfected a GFP-ARMS construct. After transfection of hippocampal neurons with GFP and GFP-ARMS, we observed a significant decrease in cell surface GluA1 in neurons expressing GFP-ARMS (Fig. 3F). Further support for the role of AMPA receptors comes from other experiments in organotypic cultures that indicated an increase in AMPA receptor-mediated currents after silencing of ARMS (Fig. 3E) and a decrease in AMPA receptor-mediated currents after overexpression of ARMS (Fig. 3G).

The increase in the accumulation of GluA1 at the cell surface expression indicates that ARMS may modulate synaptic transmission through its ability to regulate GluA1 membrane insertion. The inverse correlation of ARMS levels with GluA1 surface expression suggests that ARMS expression negatively regulates the membrane insertion of GluA1.

ARMS and GluA1 interact through transmembrane domains

A direct interaction of GluA1 with several different scaffold molecules can regulate its surface expression (Chen et al., 2000). Therefore, we assayed for a potential interaction between ARMS and GluA1. We used a protocol for interaction between transmembrane proteins that employed immunoprecipitation after protein crosslinking with the reversible crosslinking agent dithiobis-succinimidylpropionate (DSP) (Arevalo et al., 2004; Nadal et al., 2003). A strong endogenous interaction between ARMS and GluA1 could be readily detected in neurons after crosslinking and immunoprecipitation with anti-ARMS antibody (Fig. 4A). To determine the localization of this interaction, we performed immunohistochemical staining of ARMS and GluA1. Total GluA1 was detected in hippocampal neurons upon permeabilization, while cell surface levels of GluA1 were assessed under non-permeabilizing conditions using an antibody that recognizes the extracellular N-terminus of GluA1. Extensive co-localization of GluA1 and ARMS was seen in cells that had been permeabilized (Fig. 4B) while less co-localization was observed under non-permeabilizing conditions (Fig. 4B). Quantification of these data indicated that 39% of total GluA1 co-localized with ARMS, whereas only 12% of surface GluA1 co-localized with ARMS (Fig. 4C). These results suggest that GluA1 and ARMS interact mainly at intracellular locations.

To address which domains were implicated in the interaction between ARMS and GluA1, we performed transfections in HEK293 cells using different constructs of Flag-tagged ARMS and GluA1 (Fig. 4D). The interaction between ARMS and GluA1 occurred through the transmembrane domains because a truncated ARMS containing only the first and second transmembrane domains (ARMS-7) (Arevalo et al., 2004) was capable of interacting with wild-type GluA1 (Fig. 4D). Interestingly, ARMS-7 could also associate with a protein harboring a C-terminal deletion of GluA1, GluA1ΔC (Fig. 4D), suggesting that the C-terminus of GluA1, a region where many reported interactions and regulatory events take place (Malinow, 2003), was not required for the interaction with the ARMS protein.

ARMS modulates the phosphorylation of GluA1

It has been proposed that the conductance of AMPARs increases with the phosphorylation of GluA1 at Ser831 (Benke et al., 1998; Derkach et al., 1999), and trafficking of GluA1 to synapses is strongly associated with phosphorylation of Ser845 in the intracellular carboxy-terminal domain (Beique et al., 2006; Bolton et al., 2000; Esteban et al., 2003; Man et al., 2007). Therefore, we analyzed GluA1 phosphorylation of hippocampal slices from *ARMS*$^{+/-}$ and wild type mice. We found a significantly higher GluA1 phosphorylation in the *ARMS*$^{+/-}$ hippocampal slices (Fig. 5A). These data suggest that ARMS may regulate basal synaptic transmission through the AMPARs subunit GluA1.

Depletion of ARMS in cultured hippocampal neurons using ARMS shRNA lentivirus also led to an increase of GluA1 phosphorylation at Ser831 and Ser845 (Fig. 5B, left panel). Quantification of the data showed a 60% increase in the levels of Ser831 and Ser845 phosphorylation compared to control infected neurons (Fig. 5B, middle panel), whereas GluA1 expression was not affected by ARMS depletion (Fig. 5B, right panel). To assess if these effects were specific for GluA1, we tested the phosphorylation status of GluA2 at Ser880, a site that has been implicated in the removal of GluA2 receptors from the plasma membrane of granule neurons in response to long-term depression (Chung et al., 2003). Depletion of ARMS had no effect on the phosphorylation of GluA2 Ser880 as detected using specific antibodies against the phosphorylated residue (Fig. 5B, left and middle panels). Therefore, lowering ARMS is correlated with more phosphorylation of GluA1, but not GluA2 containing receptors.

ARMS modulates synaptic insertion of Ca2+-permeable GluA2-lacking AMPA receptors

Synaptic AMPARs under basal conditions contain GluA2 subunits (Bagal et al., 2005). GluA2-containing AMPARs are calcium impermeable and show a linear current-voltage relationship (Jonas and Burnashev, 1995). However, insertion of GluA2-lacking AMPARs at the synapse results in inward rectification due to polyamine block of the receptor channel pore (Bowie and Mayer, 1995; Kamboj et al., 1995) (Koh et al., 1995). Since our biochemical experiments (Fig. 3C) suggested selective insertion of GluA1 subunits at the plasma membrane after ARMS depletion, we analyzed the effect of reduced ARMS levels on the rectification index at Schaffer collateral-CA1 synapses in $ARMS^{+/-}$ and wild-type littermates. We found a significant increase in inward rectification in $ARMS^{+/-}$ mice compared to the wild-type littermates (Fig. 6B, C), indicating synaptic insertion of GluA2-lacking AMPARs in ARMS-deficient mice. Increased conductance of synaptic GluA2-lacking calcium permeable AMPA receptors (Cull-Candy et al., 2006) provides a mechanism to account for potentiated basal synaptic neurotransmission in $ARMS^{+/-}$ mice.

Discussion

Here we show that a scaffold protein, ARMS, modulates the activity of the neurons and is biochemically associated with GluA1 receptors through transmembrane domains. We find that decreasing ARMS resulted in a marked increase in basal transmission activity, which was accompanied by alterations in the phosphorylation and surface expression of GluA1 and, subsequently, AMPAR function. Therefore, ARMS can have an impact on the basal synaptic transmission through phosphorylation and surface expression of GluA1 receptors.

At the present time, the exact mechanisms that allow for greater phosphorylation of GluA1 through the ARMS protein are unknown. Delivery of AMPARs into the synapse involves soluble NSF-attachment proteins (SNAPs) as well as many other proteins, such as stargazin and other members of the TARP family, which can interact with all four subunits of AMPARs (Chen et al., 2000; Tomita et al., 2005a; Tomita et al., 2005b), PSD-95, 4.1, and SAP-97 (Chen et al., 2000; Leonard et al., 1998; Shen et al., 2000). Serine phosphorylation sites on AMPARs have been proposed to regulate the trafficking and biophysical properties of the ion channel (Boehm and Malinow, 2005; Song and Huganir, 2002). Since tyrosine phosphorylation of ARMS facilitates increases in MAP kinase activity (Arevalo et al., 2006; Arevalo et al., 2004), a signaling mechanism may explain the increased phosphorylation events involved in GluA1 trafficking (Zhu et al., 2002). This possibility will require considerably more experimentation. Alternatively, the interactions of ARMS with kinesin (Bracale et al., 2007) and other trafficking proteins, such as Ras and Rho family GEF proteins (Tada and Sheng, 2006), provide a plausible trafficking mechanism to account for increases of GluA1 distribution.

The changes in basal synaptic transmission observed in response to ARMS chronic depletion with the *ARMS*$^{+/-}$ mice were supported by other transfection experiments with truncated forms of ARMS. We expressed acutely ARMS-7, a truncated ARMS protein containing transmembrane domains that was able to interact with GluA1 subunit. We observed an increase in AMPA receptor transmission (data not shown), similar to the effect obtained with the depletion of ARMS. Previously, we have reported that ARMS is involved in refinement and maintenance of spine stability in the mature animal (Wu et al., 2009). The data obtained with the acute, short-termexpression of ARMS-7 in primary embryonic neurons indicates that ARMS has a direct effect upon glutamatergic transmission.

Chronic changes in excitatory neurotransmission in neurons frequently result in increases or decreases in the number of surface AMPA receptors (Ehlers, 2000; O'Brien et al., 1998; Turrigiano et al., 1998). Here we report that the ARMS protein can also regulate the levels of surface GluA1 receptors. Depletion of ARMS led to an increase in surface GluA1 expression with a subsequent increase in synaptic transmission, whereas over-expression of ARMS resulted in reduced cell surface GluA1. Furthermore, an increased inward rectification was observed at Schaffer collateral-CA1 synapses of *ARMS*$^{+/-}$ mice, arguing that a specific effect on GluA1 subunit may account for the increased basal synaptic transmission. In view of our results that surface GluA2 levels are not altered in response to ARMS depletion (Fig. 3C) and the increased inward rectification, it very probable that only GluA1 homomers may be affected by alteration of ARMS protein levels, although we can not rule out the potential involvement of ARMS in regulating heteromers containing GluA1. In addition, the ARMS protein is sensitive to chronic changes in synaptic strength. High levels of ARMS were observed during the initial process of synapse formation in hippocampal neurons when synaptic activity is low (Cortes et al., 2007). After maturation of hippocampal neurons, ARMS levels decrease as synapses mature. Furthermore, modulation of ARMS levels accelerates the maturation of cultured hippocampal neurons (Cortes et al., 2007) and increases basal synaptic transmission (Fig. 2A). Taken together all these data it is tempting to speculate that high ARMS levels may be seminal to keep GluA1 subunits in check early during development meanwhile the synapses are being formed and, once the synapses are assembled, reduction of ARMS levels may allow the insertion of AMPARs to create functional synapses. Additional experiments will be required to assess if ARMS may be an "activity sensor" used by neurons during development, as the maturation and formation of synapses also depends on the expression of AMPAR subunits during development.

As ARMS protein contains multiple interaction domains, it may also participate in other physiological mechanisms. Since ARMS contains protein-binding modules such as proline-rich domains known to bind SH3-containing proteins (Arevalo et al., 2004), ankyrin repeat motifs, a SAM domain, and a PDZ recognition sequence, it is likely that other synaptic proteins are associated with ARMS.

ARMS can be regulated by tyrosine phosphorylation downstream of BDNF and ephrins (Kong et al., 2001) (Arevalo et al., 2004), two classes of signaling proteins that are profoundly involved in process outgrowth and synaptic modification. Other biological functions of ARMS include neurite outgrowth and axonal transport (Arevalo et al., 2004) (Bracale et al., 2007). These observations indicate ARMS behaves as a multi-functional protein in the nervous system.

Experimental Methods

Materials

The following antibodies were used: rabbit polyclonal (Kong et al., 2001) and mouse monoclonal ARMS antibodies (gift of G. Schiavo); N-terminal GluA1 (Calbiochem), pSer831GluA1, pSer845GluA1, C-terminal GluA1, pSer880GluA2, and N-terminal GluA2 (Chemicon); tubulin and FLAG (Sigma); C-14 and PY99 (Santa Cruz); EEA1 and ribophorin (Transduction Laboratories); and GFP (Molecular Probes and Chemicon).

Plasmids

The GFP-ARMS plasmid was generated by fusing the ARMS cDNA in frame with GFP in the pEGFP-C3 plasmid from Clontech. ARMS-7 was generated by PCR amplification of nucleotide bases 991 to 1674 from rat cDNA (amino acids I331-A558). A stop codon was introduced at amino acid F828 of GluA1 to generate the GluA1ΔC construct.

The sequence 5′ gccaccaagatgagaaata 3′ of ARMS rat cDNA was used to generate ARMS shRNA using the lentiviral vector pLVTHM. Control shRNA lentivirus were generated using the sequence 5′ gcgcgctttgtaggattcg 3′ from *Euglena gracilis* chloroplast DNA between s16 S and 16 S rRNA (Kuratomi et al., 2005).

Lentivirus production

293FT cells were transfected with 9 μg of pLVTHM control shRNA or pLVTHM-ARMS shRNA together with 6 μg of psPAX2 and 5 μg of pMD.2G plasmids using 30 μl of Lipofectamine 2000 (Invitrogen). Media was changed after 6 hours and collected 48-72 hours later. The virus media was used to infect hippocampal neurons. Infected neurons can be monitored by the expression of GFP. Following infection, ARMS levels decreased by at least 80% within 3-4 days.

Cell culture

Primary cortical and hippocampal neurons were obtained from E15-16 mouse and E17-18 rat embryos. Cells were seeded in plating media (MEM, 10% FBS, 0.37% glucose, 1 mM piruvate, 2 mM glutamine, 25 U/ml penicillin, and 25 μg/ml streptomycin) overnight on poly-L-lysine-coated plates. On the next day the media was changed to Neurobasal supplemented with B-27, 0.37 % glucose, 2 mM glutamine, 25 U/ml penicillin, and 25 μg/ml streptomycin. Fluorodeoxyuridine (2.44 μg/ml) and uridine (2.44 μg/ml) were added to kill proliferating cells.

Subcellular fractionation

Subcellular fractionation was performed as described previously (Yano and Chao, 2004), using iodixanol density gradient centrifugation. Hippocampal neurons (DIV11) were homogenized using a Dounce homogenizer in buffer H (250 m*M* sucrose, 20 m*M* Tricine-NaOH, pH 7.8, 1 m*M* EDTA, 2 m*M* $MgCl_2$, with protease and phosphatase inhibitors). Membrane fractions (P2 and P3) were prepared by sequential centrifugation (800, 16,000, and 200,000×*g*) as shown in the left panel. P2 was then adjusted to 25% iodixanol (OptiPrep; Accurate, Westbury, NY) and overlaid with 20, 15, 10, and 5% iodixanol in buffer H. Gradients were centrifuged either in a SW40Ti rotor (Beckman, Fullerton, CA) at 27,000 rpm for 18 h or in a TLS55 rotor (Beckman) at 38,000 rpm for 5 h at 4°C. After gradient centrifugation, membrane fractions were collected, and equal volumes were analyzed by SDS-PAGE and immunoblotting with different antibodies.

Western blots and co-immunoprecipitations

For co-immunoprecipitation experiments, primary cultured cortical neurons (DIV 5-7) were rinsed with PBS and proteins were crosslinked with 0.5 mM dithiobis-succinimidylpropionate (DSP, Pierce) in PBS for 10 minutes as previously described (Arevalo et al., 2004; Nadal et al., 2003). Cells were lysed in a buffer containing 10 mM Tris pH 7.4, 150 mM NaCl, 2 mM EDTA, 1% NP-40, 0.2% SDS and protease and phosphatase inhibitors. Immunoprecipitated complexes were boiled for 7 minutes to cleave the crosslinked proteins. Proteins were resolved by SDS-PAGE, and western blots were performed with antibodies against different proteins.

Cell surface protein analysis

Biotinylation of cell surface proteins in cultured neurons was carried out using EZ-Link Sulfo-NHS-LC-Biotin (0.5 mg/ml) (Pierce). Biotinylated proteins were isolated using streptavidin-conjugated sepharose beads (Pierce), eluted from the beads, resolved by SDS-PAGE, and immunoblotted with the corresponding antibodies.

Immunofluorescence

Cells were fixed with 4% paraformaldehyde (PFA) for 5 min, quenched with 50 mM NH_4Cl, permeabilized where indicated, blocked with PBS containing 10% NGS, 2% FBS, and 0.2% gelatin, and incubated with primary antibodies followed by the appropriate secondary antibodies. Images were collected on a BioRad confocal microscope and processed with ImageJ (NIH). Quantification of the processed images was performed with a custom-written program in Matlab. To avoid bleed-through between channels, each channel was acquired separately in the co-localization experiments.

Electron microscopy

Adult male mice or Sprague–Dawley rats were anesthetized with sodium pentobarbital (150 mg/kg), perfused with 3.75% acrolein and 2% PFA in 0.1M phosphate buffer (PB), and processed for electron microscopy as previously described (Milner et al., 2005). For primary antibody incubation, 40-μm thick free-floating sections containing hippocampal formation and hypothalamus were incubated with affinity-purified anti-ARMS antibody (0.1-0.25 μg/ml) in 0.1% bovine serum albumin in 0.1M Tris-saline (pH 7.6) for 1 day at room temperature and an additional day at 4°C. The primary antibodies were visualized by immunogold-silver method. Sections were analyzed on a Tecnai Biotwin transmission electron microscope (FEI) equipped with an AMT digital camera.

Electrophysiology

Basal synaptic neurotransmission and PPF experiments were carried out in hippocampi from one-month-old mice. Hippocampi were cut into 300 μm transverse slices with a vibratome (Campden Instruments) and maintained at room temperature for 90 min in a brain slice keeper (Scientific Systems Design Inc.) before transferring to an interface recording chamber (Scientific Systems Design Inc.). CA1 fEPSPs were recorded at 31°C by placing both the stimulating and recording electrodes in the CA1 *stratum radiatum*. Basal synaptic neurotransmission was studied by plotting the fiber volley amplitude against slopes of fEPSPs to generate input-output relations. PPF was tested using eight inter-stimulus intervals (20, 40, 80, 120, 160, 240, 500 and 1000 ms) and defined as the second slope expressed as percentage of the first.

For the rectification index experiments, transverse hippocampal slices (300 μm) were obtained from P19 mice using a vibratome (Campden Instruments). Experiments were conducted using whole cell patch clamp recordings from CA1 pyramidal cells by

stimulating the Schaffer collaterals. The extracellular solution contained 118mM NaCl, 2.5mM KCl, 10mM glucose, 1mM NaH_2PO_4, 3mM $CaCl_2$, 2mM $MgCl_2$, 10μM bicuculline, 50μM APV and 25mM $NaHCO_3$ (osmolarity adjusted to 325 mOsm and aerated by 95% O_2/ 5% CO_2 (pH 7.4). The electrode solution contained 145mM CsCl, 10mM HEPES, 0.5mM EGTA, 5mM QX-314, 2mM Mg^{2+}-ATP, and 0.1mM spermine (Osmolarity is adjusted to 290 mOsm with sucrose, and pH is adjusted to 7.4 with CsOH.). We have obtained several points of the current-voltage relationship (holding Vm at −80, −70, −60, −50, −40, −30, −20, −10, 0, +10, +20, +30 and +40mV). The rectification index was expressed as the ratio of EPSC amplitudes: $EPSC_{-60mV}/EPSC_{+40\ mV}$ (Plant et al., 2006).

For slice culture experiments rat hippocampal slices were prepared from P4-P6 rat pups as previously described (Hayashi et al., 2000) and maintained in culture for 6–10 days. The constructs were expressed either with gene gun (overexpression of wild-type ARMS) or with lentivirus infection (ARMS shRNA). Injection of virus was performed as previously described (Hayashi et al., 2000). When virus infection was used, recordings were performed on DIV 12, 13, 14, and 15, 3-8 days (usually 5 days) following infection. Simultaneous whole-cell recordings were obtained from pairs of nearby (<50 mm apart) control and infected pyramidal neurons under visual guidance using differential interference contrast and fluorescence microscopy. The recording chamber was perfused with ACSF containing 119 mM NaCl, 2.5 mM KCl, 26 mM $NaHCO_3$, 1 mM NaH_2PO4, 11 mM glucose, 0.1 mM picrotoxin (Sigma), and 1–4 mM 2-chloroadenosine (Sigma), at pH 7.4, bubbled with a mix of 5% CO_2 and 95% O_2. 4 mM $CaCl_2$ and 4mM $MgCl_2$ were added to the ACSF for hippocampal slice cultures. All recordings were performed at 28°C. Patch pipettes (3–5 MOhm) were filled with internal solution containing: 115 mM cesium methanesulfonate, 20 mM CsCl, 10 mM HEPES, 2.5 mM $MgCl_2$, 4 mM Na_2ATP, 0.4 mM Na_3GTP, 10 mM sodium phosphocreatine, 0.6 mM EGTA, at pH 7.25 and 290 mosm. Whole-cell recordings were carried out using two Axopatch-1D amplifiers (Axon Instruments), and data were acquired and analyzed using custom software written in Igor Pro (Wavemetrics). Electrodes were placed over Schaffer collateral fibers 250 μm lateral to the recording site in hippocampal slice cultures. Stimulus intensity was adjusted so responses could typically be evoked in both cells. EPSC-amplitudes were obtained from an average of 60–80 sweeps at each holding potential. All recordings were done by stimulating two independent synaptic inputs; results from each pathway were averaged and counted as *n*=1. The AMPA-mediated EPSC was measured as peak inward current at −60 mV.

All data are reported as mean ± SEM. Statistical analysis for paired recordings used the paired t-test, while analysis for unpaired recordings used the Wilcoxon test. Significance was set to $p < 0.05$.

Acknowledgments

We thank G. Schiavo for the ARMS monoclonal antibody; E. Ziff for the GluA1 construct; D. Trono for the lentiviral plasmids; members of the Moses V. Chao, Barbara L. Hempstead, and Francis S. Lee laboratories for helpful discussions; Enrique López-Poveda for his help writing the MatLab custom-program to quantify immunofluorescence images and Belén Domínguez for continuous support. This work was supported by NIH grants (HL18974 and DA08259) to T.A.M., NIH grant (NS049442) to O.A., NIH grants (NS21072 and HD23315) to M.V.C., the Intramural Research Program of the NIH (L.T.), the Medical Scientist Training Program (S.H.W.), and by a Marie Curie International Reintegration Grant within the 7th European Community Framework Programme, by Ministerio de Ciencia e Innovacion Grant BFU2008-00162, and by Junta Castilla y León Grant SA074A08 to J.C.A. J.C.A. is a “Ramón y Cajal” Investigator from the University of Salamanca and a NARSAD 2007 Young Investigator Awardee. I.N. is a NARSAD 2008 Young Investigator and a recipient of Alzheimer’s Association New Investigator Award.

References

Arevalo JC, Pereira DB, Yano H, Teng KK, Chao MV. Identification of a switch in neurotrophin signaling by selective tyrosine phosphorylation. J Biol Chem 2006;281:1001–1007. [PubMed: 16284401]

Arevalo JC, Yano H, Teng KK, Chao MV. A unique pathway for sustained neurotrophin signaling through an ankyrin-rich membrane-spanning protein. Embo J 2004;23:2358–2368. [PubMed: 15167895]

Bagal AA, Kao JP, Tang CM, Thompson SM. Long-term potentiation of exogenous glutamate responses at single dendritic spines. Proc Natl Acad Sci U S A 2005;102:14434–14439. [PubMed: 16186507]

Beique JC, Lin DT, Kang MG, Aizawa H, Takamiya K, Huganir RL. Synapse-specific regulation of AMPA receptor function by PSD-95. Proc Natl Acad Sci U S A 2006;103:19535–19540. [PubMed: 17148601]

Benke TA, Luthi A, Isaac JT, Collingridge GL. Modulation of AMPA receptor unitary conductance by synaptic activity. Nature 1998;393:793–797. [PubMed: 9655394]

Boehm J, Malinow R. AMPA receptor phosphorylation during synaptic plasticity. Biochem Soc Trans 2005;33:1354–1356. [PubMed: 16246117]

Bolton MM, Blanpied TA, Ehlers MD. Localization and stabilization of ionotropic glutamate receptors at synapses. Cell Mol Life Sci 2000;57:1517–1525. [PubMed: 11092446]

Bowie D, Mayer ML. Inward rectification of both AMPA and kainate subtype glutamate receptors generated by polyamine-mediated ion channel block. Neuron 1995;15:453–462. [PubMed: 7646897]

Bracale A, Cesca F, Neubrand VE, Newsome TP, Way M, Schiavo G. Kidins220/ARMS is transported by a kinesin-1-based mechanism likely to be involved in neuronal differentiation. Mol Biol Cell 2007;18:142–152. [PubMed: 17079733]

Chen L, Chetkovich DM, Petralia RS, Sweeney NT, Kawasaki Y, Wenthold RJ, Bredt DS, Nicoll RA. Stargazin regulates synaptic targeting of AMPA receptors by two distinct mechanisms. Nature 2000;408:936–943. [PubMed: 11140673]

Chung HJ, Steinberg JP, Huganir RL, Linden DJ. Requirement of AMPA receptor GluR2 phosphorylation for cerebellar long-term depression. Science 2003;300:1751–1755. [PubMed: 12805550]

Cortes RY, Arevalo JC, Magby JP, Chao MV, Plummer MR. Developmental and activity-dependent regulation of ARMS/Kidins220 in cultured rat hippocampal neurons. Dev Neurobiol 2007;67:1687–1698. [PubMed: 17587220]

Cull-Candy S, Kelly L, Farrant M. Regulation of Ca2+-permeable AMPA receptors: synaptic plasticity and beyond. Current opinion in neurobiology 2006;16:288–297. [PubMed: 16713244]

Derkach V, Barria A, Soderling TR. Ca2+/calmodulin-kinase II enhances channel conductance of alpha-amino-3-hydroxy-5-methyl-4-isoxazolepropionate type glutamate receptors. Proc Natl Acad Sci U S A 1999;96:3269–3274. [PubMed: 10077673]

Ehlers MD. Reinsertion or degradation of AMPA receptors determined by activity-dependent endocytic sorting. Neuron 2000;28:511–525. [PubMed: 11144360]

Esteban JA, Shi SH, Wilson C, Nuriya M, Huganir RL, Malinow R. PKA phosphorylation of AMPA receptor subunits controls synaptic trafficking underlying plasticity. Nat Neurosci 2003;6:136–143. [PubMed: 12536214]

Hayashi Y, Shi SH, Esteban JA, Piccini A, Poncer JC, Malinow R. Driving AMPA receptors into synapses by LTP and CaMKII: requirement for GluA1 and PDZ domain interaction. Science 2000;287:2262–2267. [PubMed: 10731148]

Iglesias T, Cabrera-Poch N, Mitchell MP, Naven TJ, Rozengurt E, Schiavo G. Identification and cloning of Kidins220, a novel neuronal substrate of protein kinase D. J Biol Chem 2000;275:40048–40056. [PubMed: 10998417]

Jonas P, Burnashev N. Molecular mechanisms controlling calcium entry through AMPA-type glutamate receptor channels. Neuron 1995;15:987–990. [PubMed: 7576666]

Kamboj SK, Swanson GT, Cull-Candy SG. Intracellular spermine confers rectification on rat calcium-permeable AMPA and kainate receptors. J Physiol 1995;486(Pt 2):297–303. [PubMed: 7473197]

Koh DS, Burnashev N, Jonas P. Block of native Ca(2+)-permeable AMPA receptors in rat brain by intracellular polyamines generates double rectification. J Physiol 1995;486(Pt 2):305–312. [PubMed: 7473198]

Kong H, Boulter J, Weber JL, Lai C, Chao MV. An evolutionarily conserved transmembrane protein that is a novel downstream target of neurotrophin and ephrin receptors. J Neurosci 2001;21:176–185. [PubMed: 11150334]

Kuratomi G, Komuro A, Goto K, Shinozaki M, Miyazawa K, Miyazono K, Imamura T. NEDD4-2 (neural precursor cell expressed, developmentally down-regulated 4-2) negatively regulates TGF-beta (transforming growth factor-beta) signalling by inducing ubiquitin-mediated degradation of Smad2 and TGF-beta type I receptor. Biochem J 2005;386:461–470. [PubMed: 15496141]

Leonard AS, Davare MA, Horne MC, Garner CC, Hell JW. SAP97 is associated with the alpha-amino-3-hydroxy-5-methylisoxazole-4-propionic acid receptor GluA1 subunit. J Biol Chem 1998;273:19518–19524. [PubMed: 9677374]

Malinow R. AMPA receptor trafficking and long-term potentiation. Philos Trans R Soc Lond B Biol Sci 2003;358:707–714. [PubMed: 12740116]

Malinow R, Malenka RC. AMPA receptor trafficking and synaptic plasticity. Annu Rev Neurosci 2002;25:103–126. [PubMed: 12052905]

Man HY, Sekine-Aizawa Y, Huganir RL. Regulation of {alpha}-amino-3-hydroxy-5-methyl-4-isoxazolepropionic acid receptor trafficking through PKA phosphorylation of the Glu receptor 1 subunit. Proc Natl Acad Sci U S A 2007;104:3579–3584. [PubMed: 17360685]

Milner TA, Ayoola K, Drake CT, Herrick SP, Tabori NE, McEwen BS, Warrier S, Alves SE. Ultrastructural localization of estrogen receptor beta immunoreactivity in the rat hippocampal formation. J Comp Neurol 2005;491:81–95. [PubMed: 16127691]

Nadal MS, Ozaita A, Amarillo Y, de Miera E. Vega-Saenz, Ma Y, Mo W, Goldberg EM, Misumi Y, Ikehara Y, Neubert TA, Rudy B. The CD26-related dipeptidyl aminopeptidase-like protein DPPX is a critical component of neuronal A-type K+ channels. Neuron 2003;37:449–461. [PubMed: 12575952]

O'Brien RJ, Kamboj S, Ehlers MD, Rosen KR, Fischbach GD, Huganir RL. Activity-dependent modulation of synaptic AMPA receptor accumulation. Neuron 1998;21:1067–1078. [PubMed: 9856462]

Plant K, Pelkey KA, Bortolotto ZA, Morita D, Terashima A, McBain CJ, Collingridge GL, Isaac JT. Transient incorporation of native GluR2-lacking AMPA receptors during hippocampal long-term potentiation. Nat Neurosci 2006;9:602–604. [PubMed: 16582904]

Shen L, Liang F, Walensky LD, Huganir RL. Regulation of AMPA receptor GluA1 subunit surface expression by a 4. 1N-linked actin cytoskeletal association. J Neurosci 2000;20:7932–7940. [PubMed: 11050113]

Shin H, Hsueh YP, Yang FC, Kim E, Sheng M. An intramolecular interaction between Src homology 3 domain and guanylate kinase-like domain required for channel clustering by postsynaptic density-95/SAP90. J Neurosci 2000;20:3580–3587. [PubMed: 10804199]

Song I, Huganir RL. Regulation of AMPA receptors during synaptic plasticity. Trends Neurosci 2002;25:578–588. [PubMed: 12392933]

Tada T, Sheng M. Molecular mechanisms of dendritic spine morphogenesis. Current opinion in neurobiology 2006;16:95–101. [PubMed: 16361095]

Thiagarajan TC, Lindskog M, Tsien RW. Adaptation to synaptic inactivity in hippocampal neurons. Neuron 2005;47:725–737. [PubMed: 16129401]

Tomita S, Adesnik H, Sekiguchi M, Zhang W, Wada K, Howe JR, Nicoll RA, Bredt DS. Stargazin modulates AMPA receptor gating and trafficking by distinct domains. Nature 2005a;435:1052–1058. [PubMed: 15858532]

Tomita S, Stein V, Stocker TJ, Nicoll RA, Bredt DS. Bidirectional synaptic plasticity regulated by phosphorylation of stargazin-like TARPs. Neuron 2005b;45:269–277. [PubMed: 15664178]

Turrigiano GG, Leslie KR, Desai NS, Rutherford LC, Nelson SB. Activity-dependent scaling of quantal amplitude in neocortical neurons. Nature 1998;391:892–896. [PubMed: 9495341]

Wu SH, Arevalo JC, Sarti F, Tessarollo L, Gan WB, Chao MV. Ankyrin Repeat-rich Membrane Spanning/Kidins220 protein regulates dendritic branching and spine stability in vivo. Dev Neurobiol 2009;69:547–557. [PubMed: 19449316]

Yano H, Chao MV. Mechanisms of neurotrophin receptor vesicular transport. Journal of neurobiology 2004;58:244–257. [PubMed: 14704956]

Zhu JJ, Qin Y, Zhao M, Van Aelst L, Malinow R. Ras and Rap control AMPA receptor trafficking during synaptic plasticity. Cell 2002;110:443–455. [PubMed: 12202034]

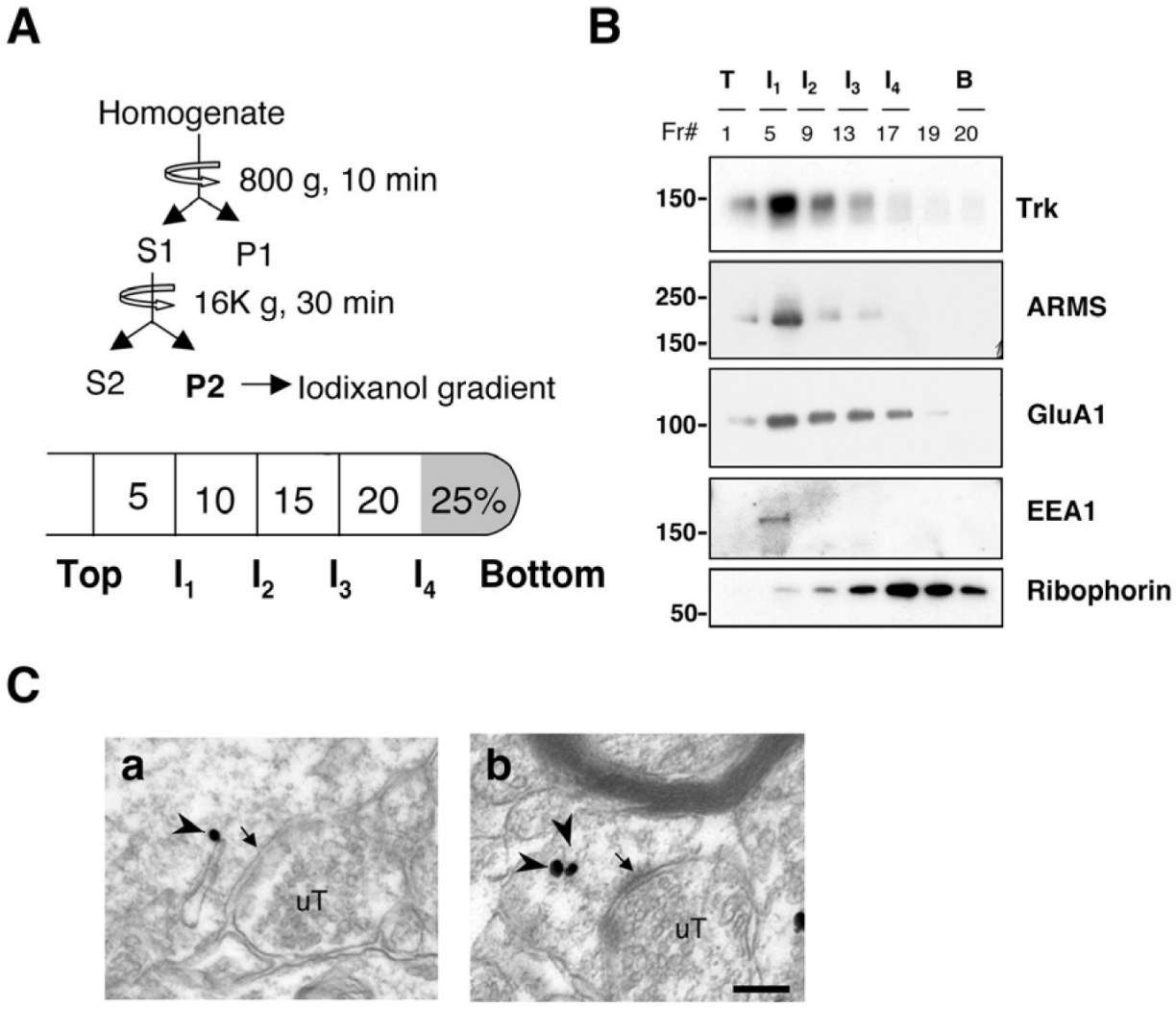

Figure 1. ARMS localizes to intracellular membranes

(A) Schematic of the protocol used to fractionate different membrane compartments from cultured hippocampal neurons (DIV 11) using iodixanol density gradient centrifugation.

(B) ARMS co-migrate with Trk receptors and GluA1 in membrane fractions. Membrane fractions from hippocampal neurons (DIV 11) were collected as described in Experimental Methods and immunoblotted for the corresponding proteins.

(C) ARMS localizes to endomembranes by electron microscopy. In *stratum radiatum* of the hippocampal CA1 region, ARMS immunogold-silver particles (arrowheads) were found in a dendritic shaft on endomembranes near a contact (arrow) from an unlabeled terminal (uT) (panel a) and in a dendritic spine on endomembranes near a synapse (arrows) from an unlabeled terminal (uT) (panel b). Scale bar, 250 nm.

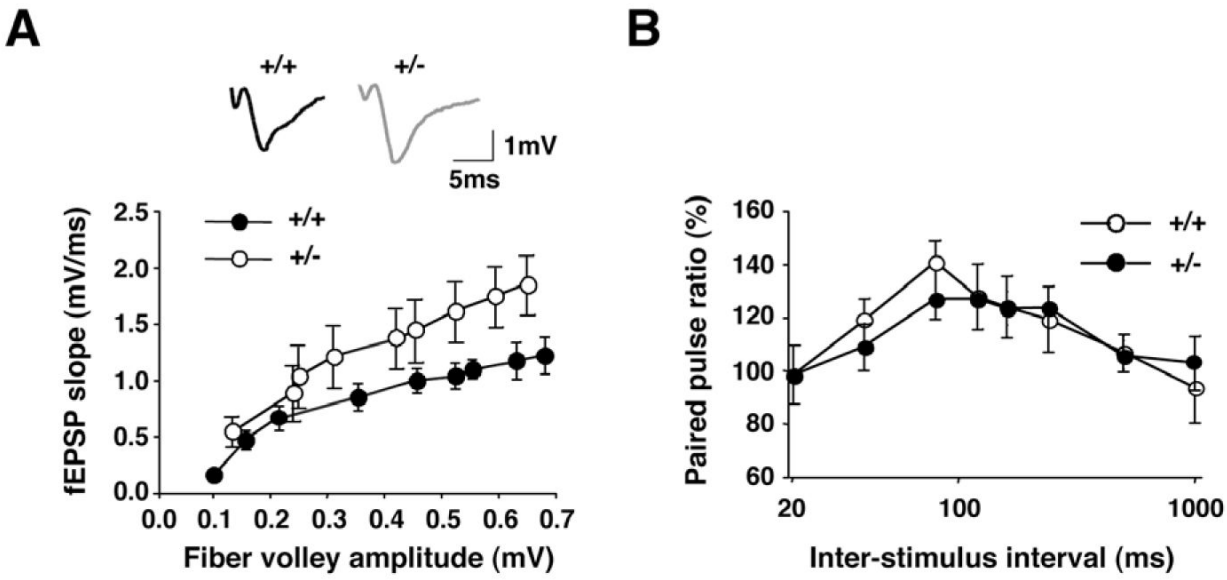

Figure 2. Increased basal synaptic transmission in *ARMS*$^{+/-}$ mice

(A) Input-output curve showing significantly higher basal synaptic neurotransmission at Schaffer collateral-CA1 synapses in *ARMS*$^{+/-}$ mice compared to wild-type mice (*n*=10 in each group; *p<0.0001; Two-way ANOVA). Inset shows examples of fEPSP recordings. **(B)** Average paired pulse ratio at Schaffer collateral-CA1 synapses in wild-type and *ARMS*$^{+/-}$ mice (*n*=7 in each group; p>0.05; Two-way ANOVA).

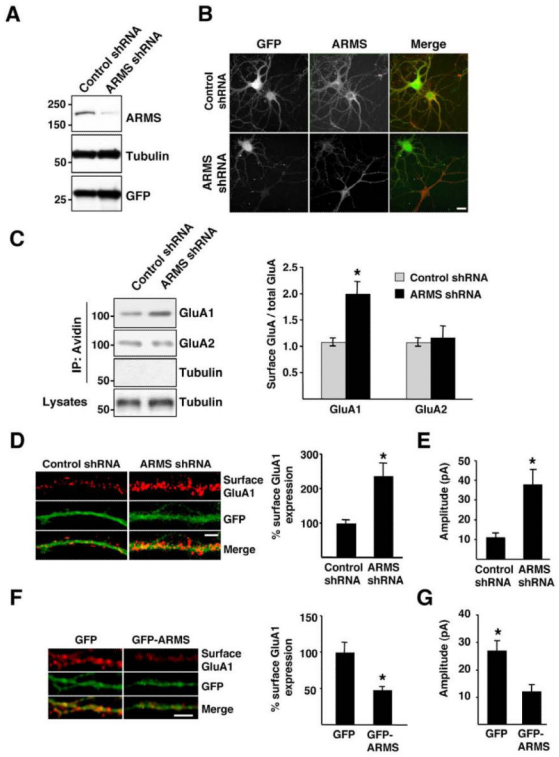

Figure 3. ARMS modulates cell surface expression of GluA1 and AMPA-mediated currents

(A) ARMS protein is specifically downregulated by lentivirus expressing ARMS shRNA. Cultured hippocampal neurons were infected at DIV 3 with control lentivirus or ARMS shRNA lentivirus and extracts were used to analyze ARMS, tubulin, and GFP expression using western blot analysis. ARMS protein was specifically downregulated in the cells infected with ARMS shRNA lentivirus while tubulin levels were unaffected. GFP expression is an indication of similar levels of viral infection.

(B) ARMS depletion using lentivirus expressing ARMS shRNA. Hippocampal neurons were infected at DIV 3 with control or ARMS shRNA lentivirus. Five days later the cells were subjected to immunofluorescence with permeabilization using ARMS and GFP antibodies. Scale bar, 10 μM.

(C) Depletion of ARMS protein increases levels of surface GluA1, but not surface GluA2 receptors. Cell surface proteins from hippocampal neurons infected with control and ARMS shRNA lentivirus were labeled with biotin and pulled down with streptoavidin. Western blot analyses were performed with GluA1, GluA2 and tubulin antibodies (left panel). Data are presented as means ± SEM of the surface GluA/total GluA ratio of 18 individual samples from 3 independent experiments (right panel) (*$p<0.05$; t-test).

(D) Increased cell surface GluA1 upon ARMS depletion. Hippocampal neurons (DIV 7) were transfected with plasmids expressing GFP and control shRNA or GFP and ARMS shRNA. Immunofluorescences were performed 48 hours later in non-permeabilized conditions with antibodies against the N-terminus of GluA1 to detect surface expression. Representative images are shown in left panels. Quantification of surface GluA1 (right panel) was performed as described in Experimental Methods (Control shRNA $n=17$; ARMS shRNA $n=9$; *$p<0.05$; t-test). Scale bar, 5 μm.

(E) Downregulation of ARMS increases AMPAR-mediated currents. The Schaffer collateral pathway was stimulated in organotypic hippocampal slices infected with lentivirus expressing with GFP-tagged control or ARMS shRNA, and GFP-positive neurons were recorded. Data are presented as mean ± SEM ($n=6$; *$p<0.05$, t-test).

(F) Neurons expressing GFP-ARMS show reduced levels of surface GluA1. GFP and GFP-ARMS transfected neurons were processed to detect surface GluA1 and quantified (right panel) as described in panel B. Representative images are shown in left panels. (GFP *n*=9; GFP-ARMS n=12; *p<0.05; t-test). Scale bar, 5 μm.

(G) Overexpression of ARMS reduces AMPAR-mediated currents. GFP and GFP-ARMS constructs were delivered to the CA1 region of organotypic brain slices, and GFP-positive neurons were recorded. Data are presented as mean ± SEM (*n*=7; *p<0.05, t-test).

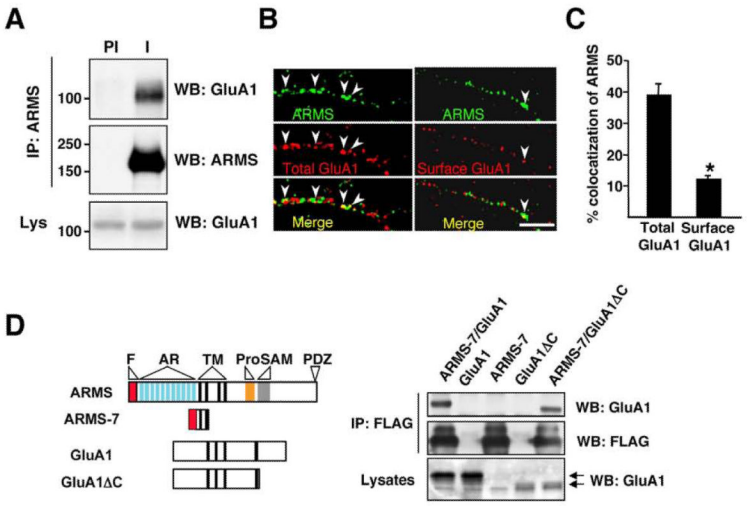

Figure 4. ARMS and GluA1 interact through transmembrane domains

(A) ARMS interacts with GluA1. Cultured cortical neurons (DIV 5-7) were crosslinked with DSP (0.5mM) for 10 minutes. Extracts were immunoprecipitated with a polyclonal ARMS antibody and immunoblotted for ARMS and GluA1. IP: immunoprecipitation; PI: preimmune serum; I: Immune serum.

(B) Intracellular GluA1 co-localizes with ARMS whereas surface GluA1 does not. Hippocampal neurons (DIV 15) were stained with N-terminus GluA1 antibody after permeabilization (total GluA1) or before permeabilization (surface GluA1) with an ARMS monoclonal antibody. Arrowheads mark areas of co-localization of ARMS and total GluA1. Scale bar, 5 μm.

(C) Quantification of ARMS and GluA1 co-localization was performed as described in Experimental Methods (*n* values are 25 and 8 for total GluA1 and surface GluA1, respectively; *$p<0.05$; total versus surface GluA1; t-test).

(D) The ARMS-GluA1 interaction is mediated by transmembrane domains. HEK293 cells were transfected with Flag-ARMS-7 and wild-type GluA1 or GluA1 lacking the C-terminus tail (GluA1ΔC). ARMS-7 was immunoprecipitated using a Flag-agarose conjugated antibody, and GluA1 association was detected using an N-terminus antibody that recognized both GluA1 proteins. F: Flag epitope; AR: Ankyrin Repeats; TM: Transmembrane domains; Pro: Proline-rich region; SAM: Sterile α-Motif; PDZ: PDZ motif.

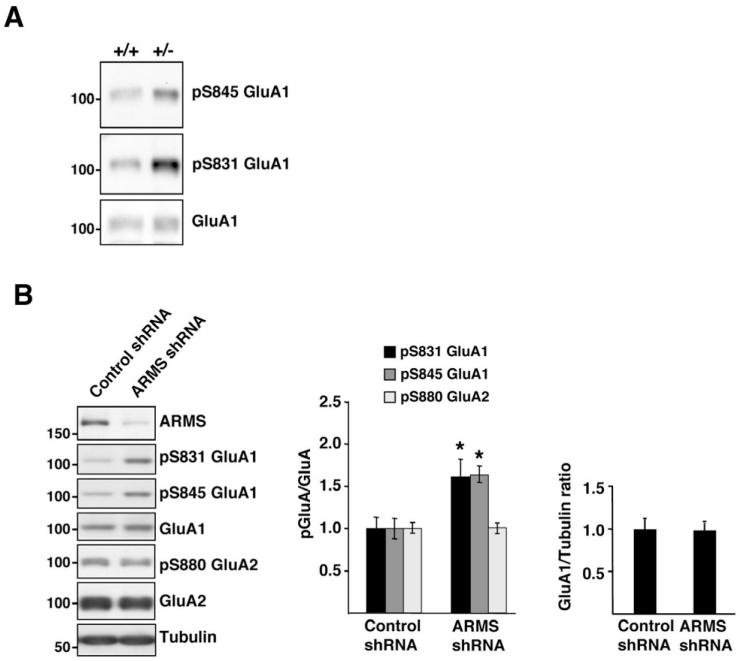

Figure 5. ARMS modulates phosphorylation of GluA1, but not GluA2

(A) GluA1 phosphorylation in hippocampal slices from wild type and *ARMS*$^{+/-}$ mice. Mouse hippocampal slices were cultured as described in Experimental Methods.

(B) GluA1 phosphorylation at Ser 831 and Ser845 is enhanced when ARMS protein is downregulated. Cultured hippocampal neurons were infected at DIV 3 with control lentivirus or ARMS shRNA lentivirus. Cells were collected at DIV 20-25 and western blot analyses were performed to assess the phosphorylation status of GluA1 at Ser831 and Ser845 and GluA2 at Ser880. A representative experiment is presented (left panel). GluA1 and GluA2 phosphorylation in response to ARMS depletion was quantified (middle panel). GluA1 expression in response to ARMS depletion was quantified (right panel). Data are presented as means ± SEM of the pGluA/GluA ratio (middle panel) and GluA1/tubulin ratio (right panel) of 18 individual samples from 3 independent experiments (*p<0.05; t-test).

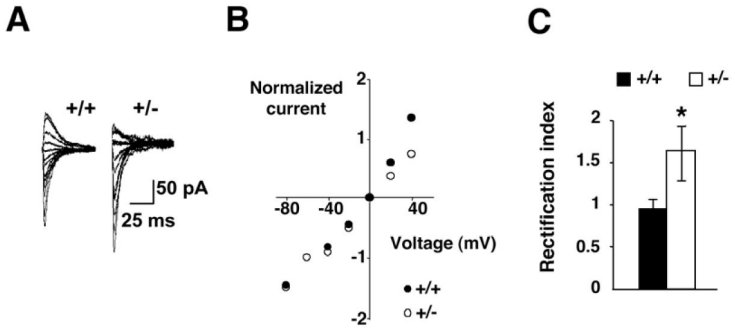

Figure 6. Increased rectification index in *ARMS*$^{+/-}$ mice

(A) Examples of synaptic currents in CA1 pyramidal neurons of wild-type and *ARMS*$^{+/-}$ mice.

(B) I-V plots for synaptic currents in wild-type and *ARMS*$^{+/-}$ mice.

(C) Average rectification index in wild-type and *ARMS*$^{+/-}$ mice (n=12 in each group; $p<0.05$; t-test).